Scientific paper

Inhibition Properties of Triton-X-100 on Ferritic Stainless Steel in Sulphuric Acid at Increasing Temperature

Regina Fuchs-Godec* and Gregor Žerjav

Faculty of Chemistry and Chemical Engineering, University of Maribor, Smetanova 17, 2000 Maribor, Slovenia

** Corresponding author: E-mail: fuchs@uni-mb.si*

Received: 12-10-2008

Dedicated to Professor Josef Barthel on the occasion of his 80th birthday

Abstract

The inhibiting action of a non-ionic surfactant of the TRITON-X series (TRITON-X-100) on stainless steel type X4Cr13 in 1.0 M H_2SO_4 solution at five different temperatures was investigated by the potentiodynamic polarisation measurements. The inhibition efficiency has been calculated in the presence and in the absence of the inhibitor. The experimental data suggest that the inhibition efficiency increases with increasing concentration of the TRITON-X-100, and decreases with the increasing temperature. Adsorption of the non-ionic surfactant used here obeys the Flory-Huggins isotherm. The thermodynamic parameters, such as, the heat of adsorption, adsorption entropy, and the adsorption free energy, have been calculated by employing thermodynamic equations. Kinetic parameters, also been evaluated.

Keywords: Non-ionic surfactants, corrosion inhibitors, sulphuric acid, Flory-Huggins adsorption isotherm

1. Introduction

Corrosion problems have received a considerable amount of attention because of the damage done on metals, especially in the high aggressive media. Sulphuric acid is commonly used in chemical cleaning and pickling to remove mill scales (oxide scales) from the metallic surface.[1] Addition of inhibitor is necessary to prevent the corrosion. Inhibitors should be effective even under severe conditions, for example, in concentrated acid and temperatures ranging from 60 to 95 °C (up to 90 °C in sulphuric acid[2–12] and up to 60 °C in hydrochloric acid[2,13–20]). The most efficient corrosion inhibitors appropriate for sulphuric acid media include heteroatoms, such as sulphur-, nitrogen- and oxygen-containing compounds. Attempts have been made to study the corrosion of various types of steels and their inhibition by different types of organic inhibitors in acid solution at higher temperatures. It was reported that azole,[21,22] pyridine[23,24] and azine[25,26] are effective corrosion inhibitors even up to 80 °C.

It is well known that surfactants can drastically change the interfacial properties and hence are used in many industrial processes such as emulsification, cosmetics, drug delivery, chemical mechanical polishing, enhanced oil recovery, and also as corrosion inhibitors.[27,28] The adsorption of surfactants on the metal surface is influenced by a number of factors.[29] The increasing temperature is one of these factors being responsible for the improving or worsening of the inhibition efficiency of the chosen surfactant. In our previous studies where anionic,[30] cationic[31,32] and non-ionic surfactants[33] were used, the highest inhibition efficiency was achieved for non-ionic surfactants.

Part of the present study is an extension of our previous work,[33] in which we investigated the inhibition abilities of two non-ionic surfactants from the TRITON-X series, that is TRITON-X-405 and TRITON-X-100. It was found that these compounds are good inhibitors in 2.0 M sulphuric acidic solutions at 25 °C. It was therefore natural to extend these studies (TRITON-X-100) to higher temperatures. The inhibition of SS of type X4Cr13 in aqueous solutions of 1.0 M H_2SO_4 was examined using the potentiodynamic polarization method. The study was performed at five temperatures ranging from 25 to 45 °C.

Thermodynamic parameters such as adsorption heat, adsorption entropy and adsorption free energy and kinetic parameters are important to explain the adsorption phenomena of inhibitor. These parameters were obtained from experimental data taken at several temperatures both in the absence and the presence of inhibitor.

2. Experimental

2. 1. Materials

The non-ionic surfactant used in the present study was of the ethoxylated octyl phenyl alcohol type (Triton-X series, Fluka products), known as TRITON-X-100, with the chemical structure C_8H_{17}–C_6H_4–$(OCH_2CH_2)_{10}$–OH. All the solutions were prepared using water obtained from a Millipore Super-Q system. The experimental concentrations were in the range from 1.0×10^{-6} – 1.0×10^{-2} M for TRITON-X-100. Cylindrically-shaped specimens were made from a rod of ferritic stainless steel of type X4Cr13 (composition in wt %: C, 0.04, S, 0.02, Si, 0.471, Cr, 13.2, Ni, 0.307, Cu, 0.213).

2. 2. Potentiokinetic Measurement

We applied the conventional three-electrode configuration to conduct the potentiodynamic studies. All the potentials were measured against the saturated calomel electrode (SCE) and the counter electrode was made from Pt. In all experiments electrochemical polarization was started 30 min after the working electrode was immersed in solution, to allow the stabilization of the stationary potential. Before each measurement, the sample was cathodically polarized at –1.0 V (SCE) for 10 min and then allowed to reach a stable open-circuit potential which was attained in about 30 min. The potentiodynamic current potential curves were recorded by automatically changing the electrode potential from –0.7 V to 0.9 V (SCE) at a scanning rate of 2 mV s^1 All the experiments were performed at the range of temperature from 25 to 45 ± 1 °C in the absence and the presence of inhibitor. A SOLATRON 1287 Electrochemical Interface was used to apply and control the potential. The data were collected using CorrWare and interpreted with CorrView software. All softwares were developed by Scribner Associates, Inc. The working electrode was ferritic stainless steel of type X4Cr13. The test specimens were fixed in a PTFE holder and the geometric area of the electrode exposed to the electrolyte was 0.785 cm^2. The metal surface was hand polished successively with emery papers of grade 400, 600, 800, 1000 and 1200. Finally, the specimen was fine polished with diamond paste to obtain a shined surface like a mirror. After polishing the working electrode, was washed up with ethanol, rinsed several times with distilled water and dried with hot air.

3. Results and Disscusions

3. 1. Electrochemical Results

The effect of the presence of TRITON-X-100 on the current–potential characteristics displayed by the polarisation curves of ferritic stainless steel type X4Cr13 in 1.0 M H_2SO_4 is presented in Fig. 1. It is clear that for a blank solution the increase of the anodic current becomes more pronounced with the rise of temperature. In presence of TRITON-X-100, the increase of anodic current is most noticeable for the highest temperature. The electrochemical parameters obtained from these polarization curves, corrosion potential (E_{corr}), corrosion current density (i_{corr}), the polarisation resistance (R_p) and the inhibition efficien-

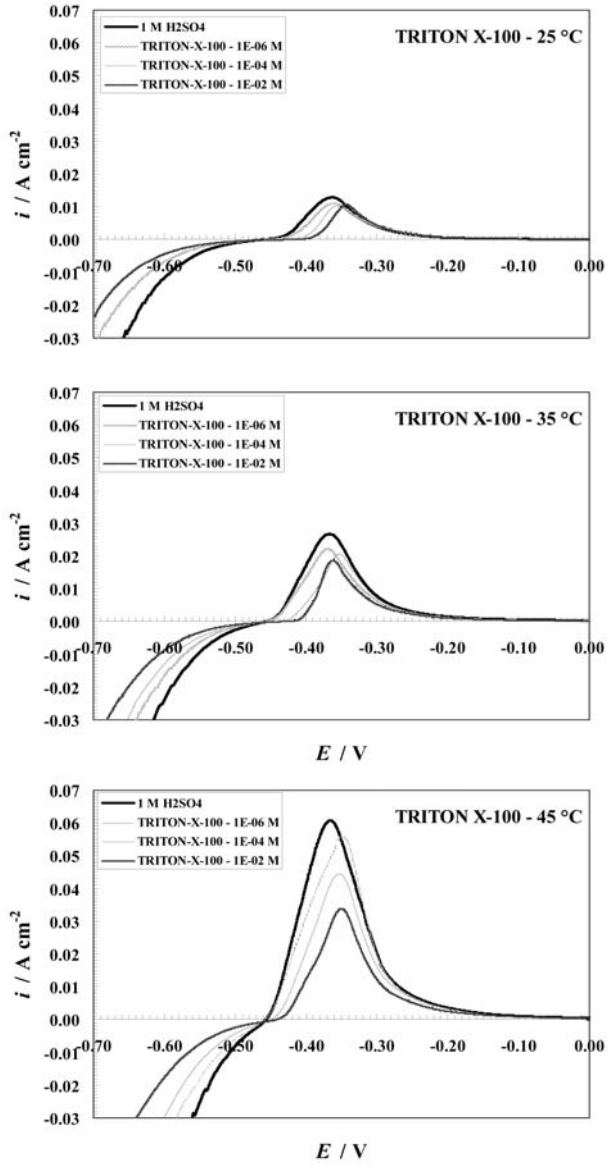

Figure 1: Temperature dependence of the anodic polarization curves of stainless steel type X4Cr13 in a mixture of 1.0 M H_2SO_4 containing various concentrations of TRITON-X-100.

cy, at various temperatures are shown in Table 1. The polarisation resistance was obtained from linear polarisation within the potential range of ±10 mV with respect to E_{corr}. Extrapolation of the Tafel line allowed us to calculate the corrosion current density i_{corr}. All the parameters were determined simultaneously by CorrView software.

The shift of E_{corr} towards more a noble value was noticed at 25 °C, and at 45 °C just at the highest used concentration of TRITON-X-100 (Figs.2). The same trend is observed in variations of the corrosion current density i_{corr}. Here, the decrease of the corrosion current was most rapid at 25 °C, and at 45 °C for the highest concentration of TRITON-X-100 added in the solution of 1.0 M H_2SO_4 (Figs. 2 and Table 1).

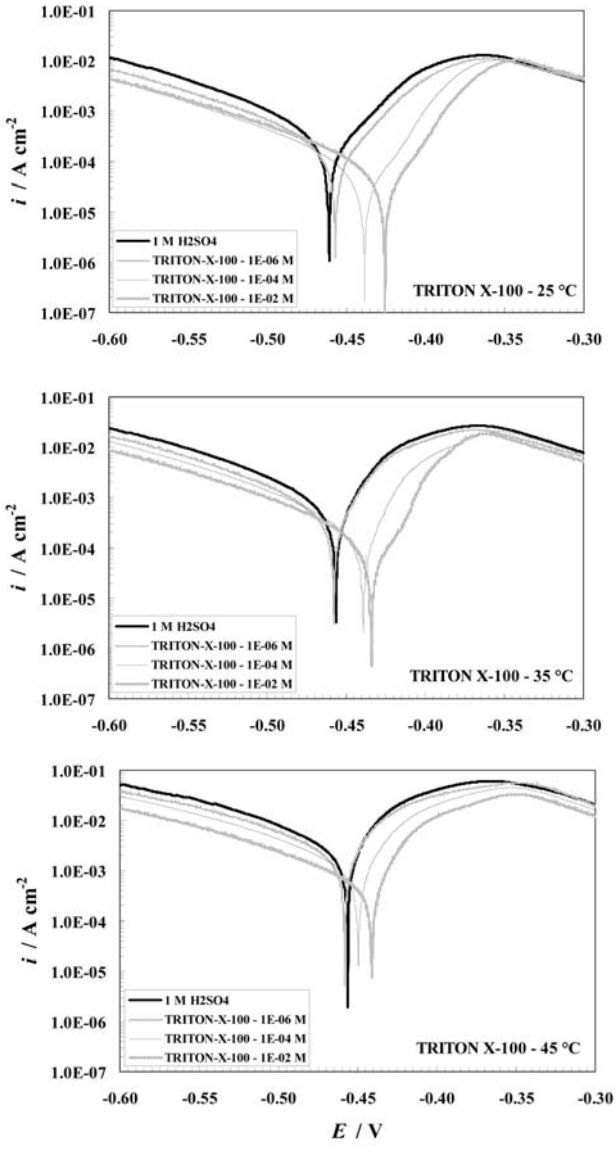

Figure 2: Influence of added TRITON-X-100 on the cathodic and anodic behaviour of stainless steel X4Cr13 in 1.0 M H_2SO_4 at different temperatures.

3. 2. Adsorption Isotherms

It is widely acknowledged that adsorption isotherms provide useful insights into the mechanism of the corrosion inhibition. Here the surface coverage θ was calculated via the kinetic parameters measured in corrosion processes as well as the polarization resistance R_p, and the corrosion current density i_{corr}, using the following equations:

$$\theta = 1 - \frac{i'_{corr}}{i_{corr}} \quad (1)$$

$$\theta = 1 - \frac{R_p}{R'_p} \quad (2)$$

The notation i_{corr}, and R_p was used for measurements without added surfactant, while the primed quantities i_{corr}' and R_p' apply when surfactant was added to the solution of 1.0 M H_2SO_4. We found that the TRITON-X-100 inhibitor behaviour in the selected temperatures range can be fitted to the Flory-Huggins adsorption isotherm[33], which has the form:

$$\log\left[\frac{\theta}{c_{inh}}\right] = \log(xK_{ads}) + x\log[1-\theta] \quad (3)$$

The calculated values of the surface coverage θ are for TRITON-X-100 in 1.0 M H_2SO_4 also reported in Table 1.

According to the Flory-Huggins model, plots of log [θ/c] versus log [1 – θ] give straight lines with a slope x and an intercept log (xK_{ads}) as showing in Fig. 3. The plot indicates that the values of x change from 7.3 to 4.8 with the increasing temperature. This suggests that one molecule of adsorbed TRITON-X-100 on the metal surface replaces more than 7 water molecules at 25 °C and reduced to less than 5 at 45 °C. The same behaviour is obtained in case when θ was evaluated from the polarisation resistance. K_{ads} is the modified adsorption equilibrium constant, which can be related to the free energy of adsorption ΔG_{ads}, given by Eq. 4:

$$K_{ads} = \frac{1}{c_{solvent}} \exp\left(\frac{-\Delta G_{ads}}{RT}\right) \quad (4)$$

Here $c_{solvent}$ is the molar concentration of solvent, which in the case of water is 55.5 M. ΔG_{ads} values calculated from Fig. 3 are negative in accordance with Eq. 4, suggesting the spontaneity of the adsorption process (Table 2).

With increasing temperature ΔG_{ads} increases (Fig. 4). One possible explanation of this effect is that the adsorption gets unfavourable with increasing temperature as the result of desorption of inhibitor from the steel surface.

Table 1: Kinetic parameters for corrosion of stainless steel type X4Cr13 obtained from potentiodynamic polarisation curves at various temperatures in 1.0 M H_2SO_4 containing various concentrations of TRITON-X-100.

1.0 M H_2SO_4 + x M TRITON-X-100	i_{corr} / (Acm^{-2})	E_{corr} / (V vs. NKE)	R_p / (Ωcm^{-2})	$\theta_{i_{corr}}$	θ_{R_p}
25 °C					
0	$3.92\ 10^{-4}$	–0.463	41.08		
$1.0\ 10^{-6}$	$1.95\ 10^{-4}$	–0.460	75.82	0.501	0.458
$1.0\ 10^{-5}$	$1.32\ 10^{-4}$	–0.457	108.40	0.665	0.621
$1.0\ 10^{-4}$	$9.43\ 10^{-5}$	–0.436	141.50	0.759	0.709
$1.0\ 10^{-3}$	$8.05\ 10^{-5}$	–0.428	186.87	0.795	0.780
$1.0\ 10^{-2}$	$5.81\ 10^{-5}$	–0.425	256.66	0.852	0.840
30 °C					
0	$7.21\ 10^{-4}$	–0.462	28.23		
$1.0\ 10^{-6}$	$3.65\ 10^{-4}$	–0.459	51.65	0.493	0.432
$1.0\ 10^{-5}$	$2.65\ 10^{-4}$	–0.455	63.52	0.632	0.555
$1.0\ 10^{-4}$	$1.94\ 10^{-4}$	–0.438	95.39	0.730	0.704
$1.0\ 10^{-3}$	$1.39\ 10^{-4}$	–0.427	144.23	0.806	0.785
1 .0 10^{-2}	$1.04\ 10^{-4}$	–0.426	155.75	0.855	0.819
35 °C					
0	$9.49\ 10^{-4}$	–0.460	19.13		
$1.0\ 10^{-6}$	$7.68\ 10^{-4}$	–0.459	24.27	0.190	0.212
$1.0\ 10^{-5}$	$4.53\ 10^{-4}$	–0.461	37.74	0.453	0.464
$1.0\ 10^{-4}$	$3.52\ 10^{-4}$	–0.440	52.69	0.628	0.637
$1.0\ 10^{-3}$	$2.81\ 10^{-4}$	–0.434	70.77	0.703	0.730
$1.0\ 10^{-2}$	$1.98\ 10^{-4}$	–0.436	92.81	0.791	0.793
40 °C					
0	$1.68\ 10^{-3}$	–0.460	11.171		
$1.0\ 10^{-6}$	$1.53\ 10^{-3}$	–0.458	12.403	0.099	0.099
$1.0\ 10^{-5}$	$1.23\ 10^{-3}$	–0.459	15.421	0.275	0.275
$1.0\ 10^{-4}$	$7.81\ 10^{-4}$	–0.443	24.293	0.540	0.540
.0 10^{-3}	$5.38\ 10^{-4}$	–0.431	35.266	0.683	0.683
$1.0\ 10^{-2}$	$3.99\ 10^{-4}$	–0.433	45.096	0.765	0.752
45 °C					
0	2.87 10–3	–0.459	4.799		
$1.0\ 10^{-6}$	$2.68\ 10^{-3}$	–0.457	5.049	0.069	0.049
$1.0\ 10^{-5}$	$2.48\ 10^{-3}$	–0.456	6.105	0.135	0.214
$1.0\ 10^{-4}$	$1.89\ 10^{-3}$	–0.448	7.042	0.342	0.318
$1.0\ 10^{-3}$	$1.01\ 10^{-3}$	–0.443	13.202	0.650	0.636
$1.0\ 10^{-2}$	$7.95\ 10^{-4}$	–0.444	17.434	0.723	0.725

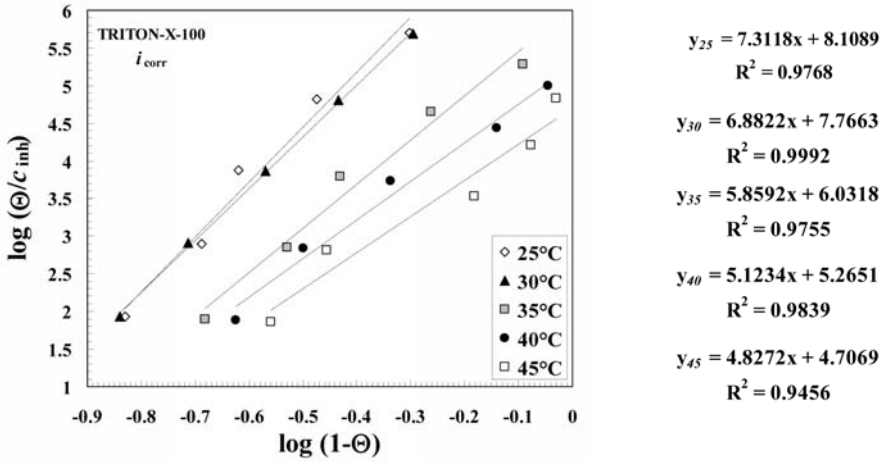

Figure 3: Flory-Huggins adsorption isotherm for TRITON-X-100 on SS type X4Cr13 in 1.0 M H_2SO_4 at different temperatures; Θ is obtained from the corrosion current density (i_{corr}). (The notation of the R^2 represents the linear correlation coefficient).

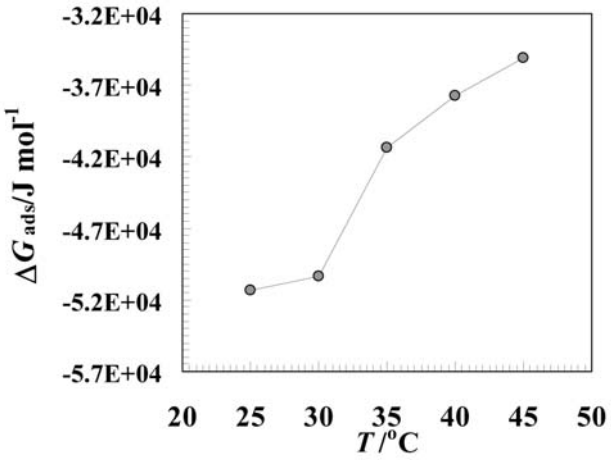

Figure 4: The free energy of adsorption ΔG_{ads} for TRITON-X-100 in 1.0 M H_2SO_4 investigated in the range of temperatures from 25 to 45 °C.

The dynamics of the anodic process at higher temperatures is more destructive. Such behaviour reduces the possibility of adsorption of organic molecules on the metal surface.

Table. 2 also gives that the adsorption equilibrium constant K_{ads} decreased with increasing temperature, which indicates that non-ionic surfactant TRITON-X-100 is easily adsorbed onto the steel surface at lower temperatures. Moreover, when the temperature is higher than 40 °C the adsorbed inhibitors tend to desorption.

Table 2: The thermodynamic parameters for adsorption of the TRITON-X-100 on the surface of SS type X4Cr13 in 1.0 M H_2SO_4 at different temperatures.

T/ °C	K_{ads} kJ mol^{-1}	ΔG_{ads} kJ mol^{-1}	ΔH_{ads} J mol^{-1}K^{-1}	ΔS_{ads}
25	1.76×10^7	–51.30		–902.56
30	8.48×10^6	–50.33		–890.88
35	1.84×10^5	–41.34	–320.41	–905.60
40	3.59×10^4	–37.76		–902.56
45	1.06×10^4	–35.13		–896.67

The adsorption heat could be calculated according to the van't Hoff equation given by Eq. 5:

$$\ln K_{ads} = -\frac{\Delta H_{ads}}{RT} + const. \quad (5)$$

Fig. 5 shows the plot of ln K_{ads} versus 1/T which gives a straight line with slope of ($-\Delta H_{ads}$ / R) and intercept ($-\Delta S_{ads}$ / R – In 55.5) . The $-\Delta H_{ads}$ value calculated from the Vant'Hoff equation is –320.41 kJ mol^{-1}. This result confirms the exothermic behaviour of the adsorption of TRITON-X-100 on the steel surface.

Knowing $\Delta G_{ads}$and ΔH_{ads} one can calculate ΔS_{ads}. According to the thermodynamic basic equation; ΔG_{ads} = $\Delta H_{ads} - T\Delta S_{ads}$, the standard adsorption entropy ΔS_{ads}can be obtained, actually calculated on the basis of the Eq. 6

$$\Delta S_{ads} = \frac{\Delta H_{ads} - \Delta G_{ads}}{T} \quad (6)$$

All the obtained thermodynamic parameters are collected in Table 2.

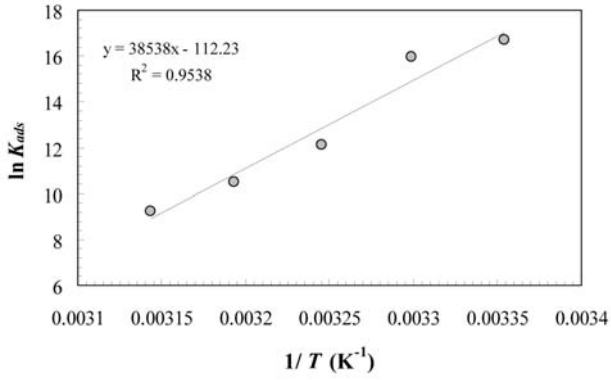

Figure 5: The relationship between ln K_{ads} and reciprocal temperature, 1/T.

The negative values of ΔS_{ads} indicate that the process of adsorption is accompanied by a decrease in entropy. We may assume that before the adsorption of the TRITON-X-100, the entropy of the system was higher (inhibitor molecules freely moved in solution). During the adsorption process inhibitor molecules were adsorbed onto the surface what decreased entropy of the system.

The corrosion reaction can be considered as an Arrhenius-type process, thus (Eq.7):

$$r = A\exp\left(\frac{-E_a}{RT}\right) \quad (7)$$

where E_a represents the apparent activation energy, R the gas constant, T the absolute temperature, A the pre-exponential factor, and r is the rate of the metal dissolution reaction. It has been reported by a number of authors [34–36] that for the acid corrosion of steel, the natural logarithm of

Table 3: The apparent activation energy and the pre-exponential factor for TRITON-X-100 of SS type X4Cr13 in 1.0 M H_2SO_4 at different concentrations of added TRITON-X-100.

1.0 M H_2SO_4 + x M TRITON-X-100	ΔEa kJ mol^{-1}	pre-expon.fact. A
0	76.12	$8.58 \times 10^{+15}$
1.0×10^{-6}	104.12	$3.33 \times 10^{+20}$
1.0×10^{-5}	116.73	$3.47 \times 10^{+22}$
1.0×10^{-4}	116.38	$2.16 \times 10^{+22}$
1.0×10^{-3}	100.92	$3.66 \times 10^{+19}$
1.0×10^{-2}	103.63	$7.81 \times 10^{+19}$

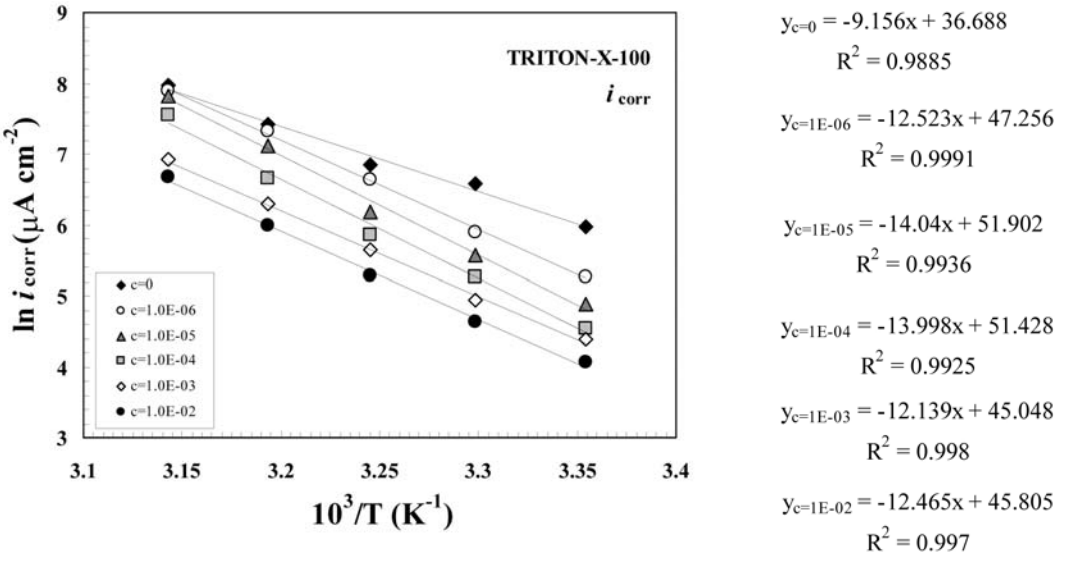

Figure 6: Arrhenius plots for TRITON-X-100 of SS type X4Cr13 in 1.0 M H_2SO_4 at different temperatures.

the corrosion rate (in g m^{-2} h^{-1}) is a linear function with 1/*T.* Since the corrosion current density i_{corr} is directly related to the corrosion rate, the apparent activation energies and pre-exponential factors at different concentrations of the inhibitor were calculated by the linear regression between ln i_{corr} and 1/*T* (Fig. 6). These results are shown in Table 3.

Some studies[37–39] showed that higher values for E_a were found in the presence of inhibitors in comparison with those obtained in the absence of it. Other studies[40,41] reported the opposite, namely, that in the presence of inhibitor the apparent activation energy was lower than in its absence. In the present study, however, it was found that with increasing concentration of TRITON-X-100 the apparent activation energy first increased, and than decreased with the increase of concentration of added nonionic surfactant. It seems that the apparent activation energy (Fig.7) is a non-monotonic function concentration.

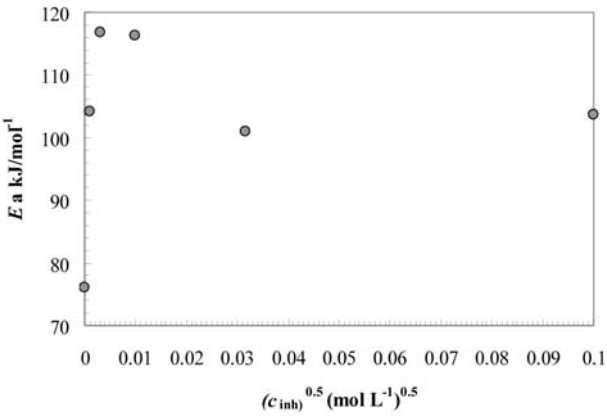

Figure 7: Dependence of the apparent activation energy on the concentration of added TRITON-X-100.

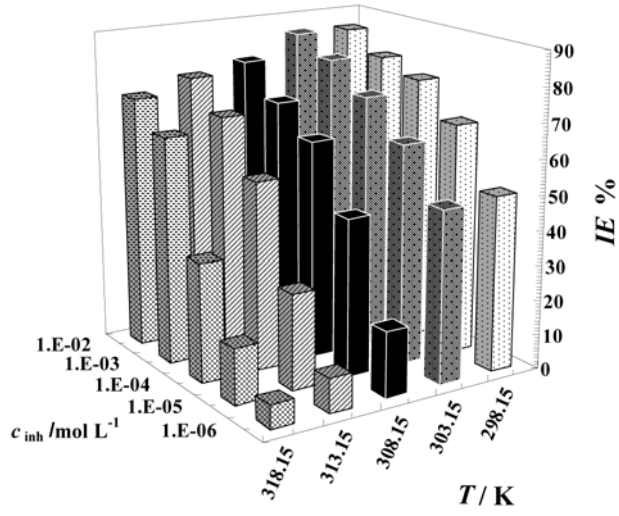

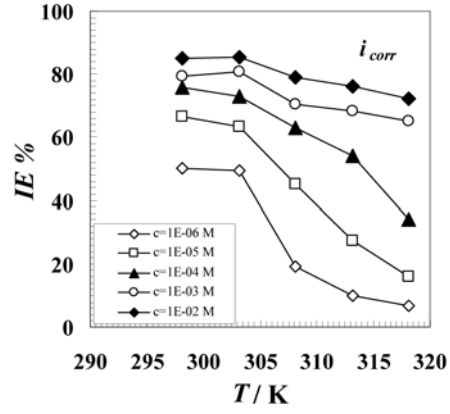

Figures 8: The corrosion inhibition efficiency (IE = θ × 100) for TRITON-X-100 of SS type X4Cr13 in 1.0 M H_2SO_4 (obtained from i_{corr}) investigated in the range of temperatures from 25 to 45 °C (289 K – 318 K) .

Moreover, the variation in the pre-exponential factors showed the same characteristic as in the case of the apparent activation energy. It increased for low concentrations of added TRITON-X-100 and started to decrease, when concentration of TRITON-X-100 was higher than c = 0.0001 M. Popova[2] et al. reported that increase of E_a in presence of the inhibitor indicates physisorption or weak chemical bonding between the inhibitor molecules and the iron surface. It could be speculated, that later decreasing of the apparent activation energy at higher inhibitor concentration leads to the chemisorptions mechanisms.

Fig.8 represents the corrosion inhibition efficiency (IE = θ × 100) for TRITON-X-100 on SS type X4Cr13 in 1.0 M H_2SO_4 as function of temperature and concentration of added non-ionic surfactant. Good inhibition efficiency of TRITON-X-100 on SS type X4Cr13 in 1.0 M H_2SO_4 was limited to the temperatures below 35 °C or for the surfactant concentration higher than c = 0.001 M (Fig. 8).

4. Conclusions

–Good inhibition efficiency of TRITON-X-100 on SS type X4Cr13 in 1.0 M H_2SO_4 was limited to temperatures below 35 °C or to surfactant concentration higher than °C = 0.001M

– The adsorption of non-ionic surfactants of TRITON-X series type on stainless steel type X4Cr13 in one molar sulphuric acid in the range of temperatures from 25 to 45 °C obeys the Flory-Huggins adsorption isotherm.

– From the electrochemical measurements and the Flory-Huggins adsorption model we concluded that TRITON-X-100 adsorbs on the stainless steel surface in 1.0 M H_2SO_4 chemically, with one molecule of the surfactant replacing more than 7 water molecules at 25 °C and reduced to less than 5 at 45 °C.

– The thermodynamic quantities obtained from this study indicate the exothermic and spontaneous behaviour of the adsorption of TRITON-X-100 on the steel surface. The negative values of ΔS^0 indicate that the process of adsorption is accompanied by a decrease in entropy.

– The apparent activation energy increased at lower concentration of added surfactant and decreased when concentration of TRITON-X-100 was higher than c = 0.0001 M. This could show on some changes in the type of adsorption process (from physisorption to chemisorptions).

5. References

1. T. Y. Soror, H. A. El-Dahan, N. G. El-Sayed Ammer, *J. Mater. Sci. Technol.* **1999**, *15, 6,* 559–562.
2. Popova, E. Sokolova, S. Raicheva, M. Christov, *Corros. Sci.* **2003**, *45,* 33–58.
3. A.K. Satpati, P.V. Ravindran, *Mater. Chem. & Phys*. **2008**, *109,* 352–359.
4. Ling-Guang Qiu, Yun Wu, Yi-Min Wang, Xia Jiang, *Corros. Sci.* **2008**, *50,* 576–582.
5. Bayol, K. Kayakırılmaz, M. Erbil, *Mater. Chem. & Phys*. **2007**, *104,* 74–82.
6. Emeka E. Oguzie, *Mater. Chem. & Phys*. **2006**, *99,* 441–446.
7. Guannan Mu, Xueming Li, Guangheng Liu, *Corros. Sci.* **2005**, *47,* 1932–1952.
8. İ. Dehri, M. Özcan, *Mater. Chem. & Phys*. **2006**, *98,* 316–323.
9. Mahmoud M. Saleh, *Mater. Chem. & Phys*. **2006**, *98,* 83–89.
10. Libin Tang, Xueming Li, Lin Li, Guannan Mu, Guangheng Liu, *Mater. Chem. & Phys*. **2006**, *97,* 301–307.
11. Libin Tang, Xueming Li, Yunsen Si, Guannan Mu, Guangheng Liu, *Mater. Chem. & Phys*. **2006**, *95,* 29–38.
12. E. E. Oguzie, G. N. Onuoha, A.I. Onuchukwu, *Mater. Chem. & Phys*. **2005**, *89,* 305–311.
13. Ehteram A. Noor, Aisha H. Al-Moubaraki, *Mater. Chem. & Phys*. **2008**, *110,* 145–154.
14. Ümit Ergun, Devrim Yüzer, Kaan C. Emregül, *Mater. Chem. & Phys*. **2008**, *109,* 492–499.
15. Xianghong Li, Shuduan Deng, Guannan Mu, Hui Fu, Fazhong Yang, *Corros. Sci.* **2008**, *50,* 420–430.
16. Ganesha Achary, H. P. Sachin, Y. Arthoba Naik, T.V. Venkatesha, *Mater. Chem. & Phys*. **2008**, *107,* 44–50.
17. K. Tebbji, N. Faska, A. Tounsi, H. Oudda, M. Benkaddour, B. Hammouti, *Mater. Chem. & Phys*. **2007**, *106,* 260–267.
18. Libin Tang, Xueming Li, Lin Li, Qing Qu, Guannan Mu, Guangheng Liu, *Mater. Chem. & Phys*. **2005**, *94,* 353–359.
19. M. Elayyachy, M. Elkodadi, A. Aouniti, A. Ramdani, B. Hammouti, F. Malek, A. Elidrissi, *Mater. Chem. & Phys*. **2005**, *93,* 281–285.
20. M. Karakuş, M. Şahin, S. Bilgiç *Mater. Chem. & Phys*. **2005**, *92,* 565–571.
21. F. Chaouket, B. Hammouti, S. Kertit, K. El Kacemi, *Bull. Electrochem.* **2001,** *17,* 311–320.
22. H. Essouffi, S. Kertit, B. Hammouti, M. Benkaddour, *Bull. Electrochem.* **2000,** *1,* 205–208.
23. Chetouani, K. Medjahed, K. E. Benabadji, B. Hammouti, S. Kertit and A. Mansri, *Prog. Org. Coat.* **2003,** *46,* 312–316.
24. A.Chetouani, K. Medjahed, K. S. Sid-Lakhdar, B. Hammouti, M. Benkaddour, A. Mansri, *Corros. Sci.* **2004,** *46,* 2421–2430.
25. Chetouani, B. Hammouti, A. Aouniti, N. Benchat, T. Benhadda, *Prog. Org. Coat.* **2002,** *45,* 373–378.
26. A.Chetouani, B. Hammouti, A. Aouniti, S. Kertit, N. Benchat, T. Benhadda, *Corros. Sci.* **2003,** *45,* 1675–1684.
27. M. Bouklah, B. Hammouti, M. Lagrenée, F. Bentiss, *Corr. Sci.* **2006**, 48, 2831–2842.
28. M. A. Migahed, *Mater. Chem. & Phys.* **2005**, 93, 48–53.
29. S. Paria, K. C. Khilar, *Adv. Colloid & Interface Science*, **2004,** *110,* 75–95.
30. R. Fuchs-Godec, V. Doleček, *Colloids Surf. A,* **2004**, *244,* 73–76.
31. R. Fuchs-Godec, *Colloids Surf. A,* **2006**, *280,* 130–139.

32. R. Fuchs-Godec, *Acta Chim. Slov.* **2007** *54, 3,* 492–506.
33. R. Fuchs-Godec, *Electrochim. Acta*, **2007**, *52,* 4974–4981.
34. Elachoruri, M. S. Hajji, M. Salem, S. Kertit, J. Aride, R. Coudert, E. Essassi, *Corrosion,* **1996,** *52,* 103–108.
35. L. B. Tang, G. N. Mu, G. H. Liu, *Corros. Sci.* **2003**, *45,* 2251–2262.
36. E. S. Ferreira, C.Giacomelli, F. C. Giacomelli, A.Spinelli, *Mater. Chem. & Phys*. **2004**, *83,* 129–134.
37. F. Bentiss, M. Traisnel, L. Gengembre and M. Lagrenée, *Appl. Surf. Sci.* **1999,** *152,* 237–249.
38. F. Bentiss, M. Lagrenée, M. Traisnel and J. C. Hornez, *Corros. Sci.* **1999**, *41,* 789–803.
39. Aouniti, B. Hammouti, M. Brighli, S. Kertit, F. Berhili, S. El-Kadiri, A. Ramdani, *J. Chim. Phys.* **1996**, *93,* 1262–1280.
40. F. Bentiss, M. Lagrenée, B. Mehdi, B. Mernari, M. Traisnel, H. Vezin, *Corrosion,* **2002,** *58,* 399–407.
41. Kertit and B. Hammouti, *Appl. Surf. Sci.* **1996**, *93,* 59–66.

Povzetek

S klasično potenciodinamsko metodo smo proučevali inhibitorski vpliv neionskega surfaktanta iz serije TRITON-X (TRITON-X-100) na feritno nerjavno jeklo X4Cr13 v 1 M raztopini žveplove VI. kisline pri temperaturah 25, 30, 35, 40, in 50 °C. Eksperimentalni podatki kažejo, da inhibicijska učinkovitost sicer narašča z naraščajočo koncentracijo, istočasno pa se začne zniževati z naraščajočo temperaturo. Izbrani neionski surfaktant se na površino kovine adsorbira v skladu s Flory–Huggins-ovo adsorpcijsko izotermo. Ocenili smo kinetične parametre, z uporabo termodinamskih enačb pa smo izračunali še klasične termodinamske parametre (ΔG_{ads}, ΔH_{ads} in ΔS_{ads}).